MRI and suspected acute pyelonephritis in children: comparison of diffusion-weighted imaging with gadolinium-enhanced T1-weighted imaging

Pierre-Hugues Vivier[1,2]; Asmaa Sallem[1]; Marion Beurdeley[3]; Ruth P Lim[4]; Julien Leroux[3]; Jérome Caudron[1,2]; Cyril Coudray[5]; Agnès Liard[3]; Isabelle Michelet[6]; Jean-Nicolas Dacher[1,2]

[1]Rouen University Hospital, CHU C. Nicolle, Service de radiopédiatrie, 1 rue de Germont, 76031 Rouen, Cedex, France.

[2]Université de Rouen, INSERM U1096, 22 boulevard Gambetta, 76183 Rouen, Cedex, France.

[3]Rouen University Hospital, CHU C. Nicolle, Service de chirurgie pédiatrique, 1 rue de Germont, 76031 Rouen, Cedex, France.

[4]Austin Health, Radiology Department, 145 Studley Rd, Heidelberg 3084, Victoria, Australia

[5]G. E. Healthcare, 24 Avenue de l'Europe CS 20529, 78457 Vélizy Villacoublay Cedex, France.

[6]Rouen University Hospital, CHU C. Nicolle, Service de pédiatrie, 1 rue de Germont, 76031 Rouen, Cedex, France.

Corresponding author:

Pierre-Hugues Vivier

Service d'imagerie pédiatrique et fœtale, INSERM U1096

CHU Charles Nicolle,

1 rue de Germont

76031 Rouen CEDEX

Tel (33) 2.32.88.64.96, Fax : (33) 2.42.88.82.35

Email: pierre-hugues.vivier@chu-rouen.fr

MRI and suspected acute pyelonephritis in children: Comparison of diffusion-weighted imaging with Gadolinium-enhanced T1-weighted imaging

ABSTRACT

Objectives: To evaluate the performance of DWI against the reference standard of gadolinium-enhanced T1-weighted imaging (Gd-T1-W) in children.

Methods: Thirty-nine consecutive patients (mean age 5.7 years) with suspected acute pyelonephritis underwent MRI including DWI and (the reference standard) Gd-T1-W . Each study was read in double-blinded fashion by two radiologists. Each kidney was graded as normal or abnormal. Sensitivity and specificity of DWI were computed. Agreement between sequences and interobserver reproducibility were calculated (Cohen κ statistic and the McNemar tests).

Results: Thirty-two kidneys (41%) had hypo-enhancing areas on Gd-T1-W images. The sensitivity and specificity of DWI were 100% (32/32) and 93.5% (43/46). DWI demonstrated excellent agreement (κ = 0.92,) with Gd-T1-W, with no significant difference (*P* = 0.25) in detection of abnormal lesions. Interobserver reproducibility was excellent with DWI (κ = 0.79).

Conclusion: DWI enabled similar detection of abnormal areas to Gd-T1-W and may provide an injection-free means of evaluation of acute pyelonephritis.

Keywords: Pyelonephritis, Kidney, Magnetic Resonance Imaging, Diffusion Magnetic Resonance Imaging, Pediatrics

Key points:

Diffusion weighted magnetic resonance imaging (DWI) can confirm acute pyelonepritis.

DWI provided comparable results to Gadolinium enhanced T1-W MRI in acute pyelonepritis.

Contrast medium injection could be avoided for diagnosing acute pyelonephritis by MRI.

MRI with T2-WI and DWI provide a fast and comprehensive diagnostic tool.

INTRODUCTION

Urinary tract infection (UTI) is frequent in children [1]. Vesicoureteral reflux (VUR), uropathies and dysfunctional elimination are the main risk factors. However, the imaging workup remains controversial. Ultrasound is routinely the first imaging investigation but has imperfect diagnostic sensitivity and specificity (48% and 66% respectively) [2]. ^{99m}Tc-dimercaptosuccinic acid (DMSA) renal scintigraphy is considered the reference technique to demonstrate acute pyelonephritis (APN) but is not recommended in routine practice according to recent guidelines from the American Academy of Pediatrics [1]. ^{99m}Tc-DMSA scintigraphy has several drawbacks, in particular, exposure to ionising radiation, relatively poor spatial resolution, and limited availability. It may be difficult to obtain the emergency setting in many centres, and furthermore is no longer available in many countries. It is also a relatively slow technique, with a delay of 3 hours required after tracer injection before imaging can be performed. Some studies have shown the potential applicability of MRI for pyelonephritis in children [3-5]. Combined guidelines from the European Society of Uroradiology (ESUR) and the European Society of Pediatric Radiology (ESPR) state that MRI could help in cases of unclear diagnosis of APN [6].

Diffusion-weighted imaging (DWI) has been routinely performed in uroradiology for a decade [7-9]. Potential strengths of DWI in assessing the paediatric population are: no requirement for intravenous access and contrast medium administration; and an ability to obtain sharp images when respiratory-triggering is applied [10]. DWI is known to be of great value in cases of suspected pyelonephritis by showing hyper-intense abnormal areas [9; 11-14]. However, to our knowledge, its diagnostic performance has not been scientifically evaluated. The goal of our study was to evaluate the performance of DWI against the reference standard of gadolinium-enhanced T1-weighted imaging (Gd-T1-W) in children referred for suspected APN. As this study was not performed in patients with a clear-cut diagnosis of APN, the purpose was not to assess the value of DWI for the diagnosis of APN but rather to know if contrast medium injection could be replaced by a DWI sequence.

MATERIALS AND METHODS

Patients

The ethics committee granted exempt status for this study and waived the need for informed consent. Subjects were identified by a database search for children aged 6 months to 16 years examined for possible APN with MRI between January 2010 and March 2012 at our university hospital. MRI was performed for the clinical indication of suspected pyelonephritis, encompassing patients with positive urine culture with normal ultrasound, doubtful urine culture, antibiotic prescription before urinalysis, or unfavourable clinical response after 48 h of antibiotics.

MR Imaging

All patients underwent MRI at 1.5-T (Signa HDxt; General Electric, Milwaukee, WI, USA). Light sedation (oral hydroxyzine: 2mg/kg to a maximum dose of 60 mg 45 minutes before scanning) was performed following our local protocol. Our routine MR protocol is described as follows. After scout images, T2-weighted images were performed in oblique coronal and axial planes. Then, DWI images were acquired in the same planes.. An oblique coronal dynamic T1-weighted sequence was then performed for 90 s starting after injection of a bolus of 0.05 mmol/kg gadoterate meglumine (Dotarem; Guerbet, Paris, France). Oblique coronal T1-weighted sequences were finally performed. MR protocol parameters are displayed in Table 1.

Analysis of Findings

All images were independently interpreted by two readers (A.S.; P.H.V., with 2 and 9 years of experience respectively in paediatric kidney MRI). Each examination was divided into two individual sequences: DWI and Gd-T1-W images (including coronal dynamic images and delayed images at 90 s). The anonymised image sets were examined in random order at different time points (all of one sequence type at a time) each separated by at least 1 month, to minimise recall bias. For DWI, hyper-intensities were recorded only if they were present at the same location on both coronal and axial images.

The Gd-T1-W images (dynamic and late phase images) were considered our reference method for identifying an area of pyelonephritis [3; 15; 16]. Any abnormality (hypointensity) at Gd-T1-W on any image at any time point was considered a positive finding. Readers recorded abnormality as being present or absent within each kidney for each sequence. For more detailed analysis, readers were also asked to identify the presence or absence of pyelonephritis in each of three zones per kidney; the upper, middle and lower thirds. The middle third was located between the upper and lower renal lips. After data analysis, any discrepant results between readers were resolved by consensus for each sequence, and discrepancies between sequences were reviewed by both readers.

Overall image quality was assessed on a three-point scale, where a score of 1 = excellent quality, a score of 2 = sufficient quality to make a diagnosis (slight motion artefacts), a score of 3 = non-diagnostic images (anatomical regions unassessable, severe motion artefacts).

Statistical Analysis

Image quality of the two sequences was compared using a Wilcoxon signed rank test. κ statistics and the McNemar test were used to measure agreement between MR findings. For κ, values were defined as [5]: excellent, $\kappa > 0.75$; fair to good, $\kappa = 0.40–0.75$; and poor, $\kappa < 0.40$. Sensitivities, specificities, positive and negative predictive values and 95% confidence intervals for detecting renal abnormality were calculated. Inter-observer reproducibility was measured by the κ statistic and the McNemar test. P values less than 0.05 were considered significant. Commercially available software (MedCalc Software; MedCalc, Mariakerke, Belgium) was used for statistical analysis.

RESULTS

Thirty-nine consecutive paediatric patients (mean age 5.7 years ; min 0.5– max 15.0) were included (Table 2), with no patient exclusions. Both observers ranked the image quality as 1.24 (± 0.26) for DWI images and 1.46 (± 0.40) for Gd-T1-W images. The quality of Gd-T1-W images was scored significantly poorer than that of DWI images ($P = 0.006$). No images for any of the two sequences were considered non-diagnostic (score = 3) by either observer.

After final evaluation by both observers 28/39 patients (72%) had abnormalities on Gd-T1-W images. Bilateral abnormalities were present in 4/28 patients (14%). Therefore, a total of 32 kidneys showed regions of decreased signal intensity. Out of the 234 (3 x 39 x 2) renal zones, 79/234 (34%) were judged abnormal. There was high interobserver agreement, with only 1 kidney judged normal by one observer and abnormal by the other, and 12 zones (5%) rated differently before re-evaluation by consensus.

T2 abnormalities corresponded to hyper- or hypointensities. DWI abnormalities were always hyperintense on b-1,000 images and associated with reduced signal intensity on ADC maps (Fig. 1). Hyperintensities observed on DWI were thus not related to a T2 shine-through effect but to a real decrease in water diffusion.

Diffusion-weighted images demonstrated excellent agreement with Gd-T1-W images (κ = 0.92), and the detection of abnormal lesions was not significantly ($P \geq 0.2266$) different from Gd-T1-W images (Table 3). DWI images provided excellent sensitivity (≥ 96.2 %), specificity (≥ 93.5 %) and interobserver reproducibility ($\kappa \geq 0.79$; Table 4).

Diffusion-weighted images were read as abnormal in more renal zones than were Gd-T1-W images (84 vs. 79). Of 234 zones, 11 (4.7 %) were discrepant between DWI and Gd-T1-W images. These discrepancies were analysed by both observers in consensus to try to explain the mismatches. Eight zones were abnormal with DWI and normal with Gd-T1-W images. Four of these discrepancies were explained by small lesions on DWI that could be seen in retrospect on Gd-T1-W images at the second reading (Fig. 2). In 2 patients, DWI abnormalities were clearly visible but not on Gd-T1-W images which were considered of suboptimal quality. In the other 2 patients, both DWI and Gd-T1-W images were suboptimal owing to motion. Three zones were abnormal on Gd-T1-W and normal on DWI images. Two of these were probably false-positive on Gd-T1-W sequence (our reference method): one was considered to represent bowel gas-related artefact by both observers at the second reading and the other poor image quality. The third was related to the poor image quality of DWI. Finally, after consensus analysis, at least 8 of the 11 discrepant zones might be considered as correctly rated on DWI images.

Five patients had abscesses or microabscesses. They systematically appeared as areas of hyperintensity with a hypointense periphery on T2-W images, hyperintensity relative to adjacent areas of nephritis on DWI with restricted apparent diffusion coefficient, and hypointensity on Gd-T1-W at any time during the 2 min after contrast medium injection (Fig. 3).

DISCUSSION

To our knowledge, although DWI is commonly used in the setting of pyelonephritis, this study is the first to assess its performance in children. DWI provided comparable results to Gd-T1-W imaging, our reference technique, with excellent interobserver reproducibility between two readers with a variable level of experience. Furthermore, the analysis of the 11 discrepant zones between DWI and Gd-T1-W results were considered to be better classified by DWI. This has exciting implications for the paediatric population studied in our work. MRI can be easily performed without the need for intravenous access or injection. Anatomical images provided by T2-W images in association with DWI could provide a comprehensive diagnostic assessment in approximately 20 min, including patient set-up and reference imaging, comparing favourably with the total examination time of ^{99m}Tc-DMSA scintigraphy.

The quality of DWI images was ranked significantly (*P* = 0.006) better than the Gd-T1-W images in our study. This is likely because volumetric Gd-T1-W images may suffer from respiratory motion artefact. Owing to temporal resolution constraints imposed by contrast kinetics, and greater sensitivity of 3D imaging to motion artefact, the clinical standard Gd-T1-W is less amenable to respiratory triggering. This is contrary to 2D T2-W and DWI sequences, where there are no such constraints of contrast timing. Gd-T1-W images at 90 s were performed with breath-holding when possible, but this was not feasible in most children who were too young to follow breath-hold instructions.

The duration of restricted water diffusion after acute pyelonephritis remains unknown. This issue is a major drawback of ^{99m}Tc-DMSA scintigraphy which cannot differentiate chronic scarring from APN. Of interest, MRI with T1-W and T2-W morphological sequences readily depicts mature renal scarring [3; 5; 17; 18]. As a result, regardless of the duration of restricted diffusion abnormalities, unenhanced MRI combining morphological sequences and DWI should be a comprehensive examination in the setting of APN. Moreover MRI has a much better spatial resolution than scintigraphy and does not expose to ionising radiation to which children are particularly sensitive. The effective dose of ^{99m}Tc-DMSA scintigraphy is approximately 1 mSv regardless of the age of the child [19; 20].

Our study had limitations. This was a retrospective study with non-uniform imaging indications. We did not perform MRI in children younger than 6 months as ADC is known to be reduced in this age group [21], and kidneys receive less than 5% of the cardiac output compared with 20% in adults.

We did not use a gadolinium-enhanced inversion-recovery sequence [4; 5] for post-contrast evaluation of the kidneys. The quality of negative enhancement of normal renal tissue (tissue nulling) is dependent on the contrast medium concentration and chosen TI value with this technique [5]. Renal T1 values change dramatically over the first few minutes after contrast medium injection [22; 23]. As our clinical MR platform was not equipped with a TI scout sequence, the choice of a correct TI value could not be readily determined, and our experience with fixed TI values to null normal renal tissue when setting up our MR protocol for APN did not provide a satisfactory result. However, we used a widely available post-contrast technique that is easy to perform and interpret in clinical practice [3; 15; 16].

Magnetic resonance findings were not compared with those of ^{99m}Tc-DMSA renal scintigraphy, the reference imaging investigation for APN. However, the goal of this preliminary study was not to assess the value of DWI for the diagnosis of APN, but to know if contrast medium injection could be replaced by a DWI sequence. Data provided by the two MR sequences did not show significant differences ($P \geq 0.22$) based on 234 renal zones. These results suggest that contrast medium injection is not mandatory in this setting.

In conclusion, we have shown that DWI is an easily implemented and well-tolerated technique that is comparable to Gd-MRI for identifying renal abnormalities in children with suspected acute pyelonephritis. Advantages include the absence of intravenous puncture, which would make MRI more acceptable to both children and their parents. The avoidance of a contrast medium injection also improves cost-effectiveness and out-of-hours availability when fewer staff are present. Based on our results, we plan to perform a prospective study to compare the diagnostic value of MR imaging including DWI against ^{99m}Tc-DMSA scintigraphy.

REFERENCES

1 Roberts KB (2011) Urinary tract infection: clinical practice guideline for the diagnosis and management of the initial UTI in febrile infants and children 2 to 24 months. Pediatrics 128:595-610

2 Preda I, Jodal U, Sixt R, Stokland E, Hansson S (2010) Value of ultrasound in evaluation of infants with first urinary tract infection. J Urol 183:1984-1988

3 Grattan-Smith JD, Little SB, Jones RA (2008) Evaluation of reflux nephropathy, pyelonephritis and renal dysplasia. Pediatr Radiol 38 Suppl 1:S83-105

4 Lonergan GJ, Pennington DJ, Morrison JC, Haws RM, Grimley MS, Kao TC (1998) Childhood pyelonephritis: comparison of gadolinium-enhanced MR imaging and renal cortical scintigraphy for diagnosis. Radiology 207:377-384

5 Majd M, Nussbaum Blask AR, Markle BM et al (2001) Acute pyelonephritis: comparison of diagnosis with 99mTc-DMSA, SPECT, spiral CT, MR imaging, and power Doppler US in an experimental pig model. Radiology 218:101-108

6 Riccabona M, Avni FE, Blickman JG et al (2008) Imaging recommendations in paediatric uroradiology: minutes of the ESPR workgroup session on urinary tract infection, fetal hydronephrosis, urinary tract ultrasonography and voiding cystourethrography, Barcelona, Spain, June 2007. Pediatr Radiol 38:138-145

7 Fukuda Y, Ohashi I, Hanafusa K et al (2000) Anisotropic diffusion in kidney: apparent diffusion coefficient measurements for clinical use. J Magn Reson Imaging 11:156-160

8 Toyoshima S, Noguchi K, Seto H, Shimizu M, Watanabe N (2000) Functional evaluation of hydronephrosis by diffusion-weighted MR imaging. Relationship

between apparent diffusion coefficient and split glomerular filtration rate. Acta Radiol 41:642-646

9 Verswijvel G, Vandecaveye V, Gelin G et al (2002) Diffusion-weighted MR imaging in the evaluation of renal infection: preliminary results. JBR-BTR 85:100-103

10 Taouli B, Sandberg A, Stemmer A et al (2009) Diffusion-weighted imaging of the liver: comparison of navigator triggered and breathhold acquisitions. J Magn Reson Imaging 30:561-568

11 Chan JH, Tsui EY, Luk SH et al (2001) MR diffusion-weighted imaging of kidney: differentiation between hydronephrosis and pyonephrosis. Clin Imaging 25:110-113

12 Leeuwenburgh MM, Wiarda BM, Bipat S et al (2012) Acute Appendicitis on Abdominal MR Images: Training Readers to Improve Diagnostic Accuracy. Radiology 264:455-463

13 Thoeny HC, De Keyzer F (2011) Diffusion-weighted MR imaging of native and transplanted kidneys. Radiology 259:25-38

14 Thoeny HC, De Keyzer F, Oyen RH, Peeters RR (2005) Diffusion-weighted MR imaging of kidneys in healthy volunteers and patients with parenchymal diseases: initial experience. Radiology 235:911-917

15 Martina MC, Campanino PP, Caraffo F et al (2010) Dynamic magnetic resonance imaging in acute pyelonephritis. Radiol Med 115:287-300

16 Stunell H, Buckley O, Feeney J, Geoghegan T, Browne RF, Torreggiani WC (2007) Imaging of acute pyelonephritis in the adult. Eur Radiol 17:1820-1828

17 Kavanagh EC, Ryan S, Awan A, McCourbrey S, O'Connor R, Donoghue V (2005) Can MRI replace DMSA in the detection of renal parenchymal defects in children with urinary tract infections? Pediatr Radiol 35:275-281

18 Kovanlikaya A, Okkay N, Cakmakci H, Ozdogan O, Degirmenci B, Kavukcu S (2004) Comparison of MRI and renal cortical scintigraphy findings in childhood acute pyelonephritis: preliminary experience. Eur J Radiol 49:76-80

19 Smith T, Evans K, Lythgoe MF, Anderson PJ, Gordon I (1996) Radiation dosimetry of technetium-99m-DMSA in children. J Nucl Med 37:1336-1342

20 Vestergren E, Jacobsson L, Lind A, Sixt R, Mattsson S (1998) Administered activity of 99Tcm-DMSA for kidney scintigraphy in children. Nucl Med Commun 19:695-701

21 Jones RA, Grattan-Smith JD (2003) Age dependence of the renal apparent diffusion coefficient in children. Pediatr Radiol 33:850-854

22 Rohrschneider WK, Haufe S, Wiesel M et al (2002) Functional and morphologic evaluation of congenital urinary tract dilatation by using combined static-dynamic MR urography: findings in kidneys with a single collecting system. Radiology 224:683-694

23 Vivier PH, Storey P, Rusinek H et al (2011) Kidney function: glomerular filtration rate measurement with MR renography in patients with cirrhosis. Radiology 259:462-470

TABLES

TABLE 1. Typical parameters of standard magnetic resonance urography (MRU) protocol with our 1.5-T MRI

	T2-W coronal	T2-W axial	DWI coronal	DWI axial	Gd-T1-W† Coronal Dynamic	Gd-T1-W† Coronal
Type	FSE	FSE	Echoplanar SE	Echoplanar SE	FSPGR	FSPGR
2D/3D	2D	2D	2D	2D	3D	3D
TR (ms)	8571	10714	7200	8276	2.44	3.8
TE (ms)	120	120	72	72	1.13	1.76
Flip angle (°)	90	90	90	90	12	15
B value (s/mm^2)	-	-	0, 1000	0, 1000	-	-
Bandwidth (kHz)	50	50	250	250	125	62.5
Parallel imaging*	-	+	+	+	-	+
Acceleration factor		2	2	2		2
Fat saturation	+	+	-	-	-	+
Number of sections	19	35	19	35	40	40
Section thickness (mm):	4	4	5	6	4	4
Spacing between sections (mm)	4.5	4.5	5	5	2	2
FOV	370x300	370x300	400x360	400x200	400x280	400x360
Acquisition matrix	352 x 192	352 x192	80 x128	80 x 128	192 x 160	240 x 240
Interpolated matrix	512 x 512	512 x 512	256 x 256	256 x 256	512 x 512	512 x 512
Respiratory triggering	+	+	+	+	-	-
Acquisition duration	35 s	40 s	125 s	150 s	4.6 s x 20	13 s
Effective acquisition duration (depending on respiratory cycle)	60 s	70 s	240 s	300 s	91 s	13 s

† LAVA: Liver Acquisition with Volume Acceleration. *ASSET: Array Spatial Sensitivity.

FOV: Field of view; FSE: Fast Spin Echo; FSPGR: Fast SPoiled Gradient Recalled; SE: Spin Echo

TABLE 2. Patient Characteristics

Number of patients	39
Indications for MRI	
ATB before urinalysis	10
Normal ultrasound	15
Doubtful urinalysis	9
Unfavourable response to ATB	5
Males	12 (31 %)
Median age (min–max)	6.2 years (0.5–15.0)
Mean peak temperature (min-max)	39.0°C (38.0– 40.0)
Mean CRP (min-max)	144 mg/dL (10– 456)
Leucocytosis (min-max)	16.0 G/dL (4.4–28.0)
Positive urine culture	20 (51 %)
E. Coli	12 (60 %)
Other organisms	8 (40 %)

ATB: Antibiotics

TABLE 3. Detection of renal abnormalities with T2-W versus DWI

		DWI	
		+	-
	Gd-T1-W		
	+	32	0
	-	3	43
Per kidney	Sens. (95% CI)	100% (89.1 – 100)	
(*n* =78)	Spe. (95% CI)	93.5% (82.1 – 98.6)	
	PPV (95% CI)	91.4% (76.9 – 98.2)	
	NPV (95% CI)	100% (91.8 – 100)	
	κ value* (95% CI)	0.92 (0.83 - 1.00)	
	P value†	0.2500	
		+	-
	Gd-T1-W		
	+	76	3
	-	8	147
Per zone	Sens. (95% CI)	96.2% (89.3 – 99.2)	
(*n* =234)	Spe. (95% CI)	94.8% (90.1 – 97.7)	
	PPV (95% CI)	90.5% (82.1 – 95.8)	
	NPV (95% CI)	98.0% (94.3 – 99.6)	
	κ value* (95% CI)	0.92 (0.87 - 0.98)	
	P value†	0.2266	

Sens. = sensibility, Spe. = specificity, PPV = positive predictive value, NPV = negative predictive value, 95% CI = 95% confidence interval

* excellent agreement, κ >0.75; fair to good agreement, κ = 0.40–0.75; poor agreement, κ <0.40

†Calculated with the McNemar test

TABLE 4. Inter-observer reproducibility

		κ value*	95% CI	*P* value†
DWI	per kidney	0.79	0.66 – 0.93	0.73
	per kidney zone	0.86	0.79 – 0.93	1.00
Gd-enhanced T1-W	per kidney	0.97	0.92 – 1.00	1.00
	per kidney zone	0.88	0.82 – 0.95	0.15

* Excellent agreement, κ >0.75; fair to good agreement, κ = 0.40 – 0.75; poor agreement, κ <0.40

†Calculated with the McNemar test

FIGURE LEGENDS

Fig. 1. Example of MR images in a 9-year old boy. Minimal abnormality is visible on T2-W images considered normal by observers during independent sequences readings (A, B). DWI images (b=1000 s/mm^2) (C, E) show a conspicuous hypersignal at the right upper pole corresponding to a restricted diffusion area on the ADC map (D). A sharp perfusion defect is visible at the same location on Gd-T1-W images at the arterial phase (F), tubular phase (G), and excretory phase (H).

Fig. 2. Example of discrepancy between DWI and Gd-T1-W. A small lesion (arrow) is visible on DWI only (B, C) at the first reading and also seen on T2-W (A) and Gd-T1-W (D) images at the second reading aiming at understanding discrepancies.

Fig.3. Small abscess in the right upper pole.

(A) Axial T2-W image, (B) axial DWI image, (C) axial ADC map, (D) coronal T2-W image, (E) coronal DWI image, (F) coronal Gd-T1-W image.

Arrow: abscess

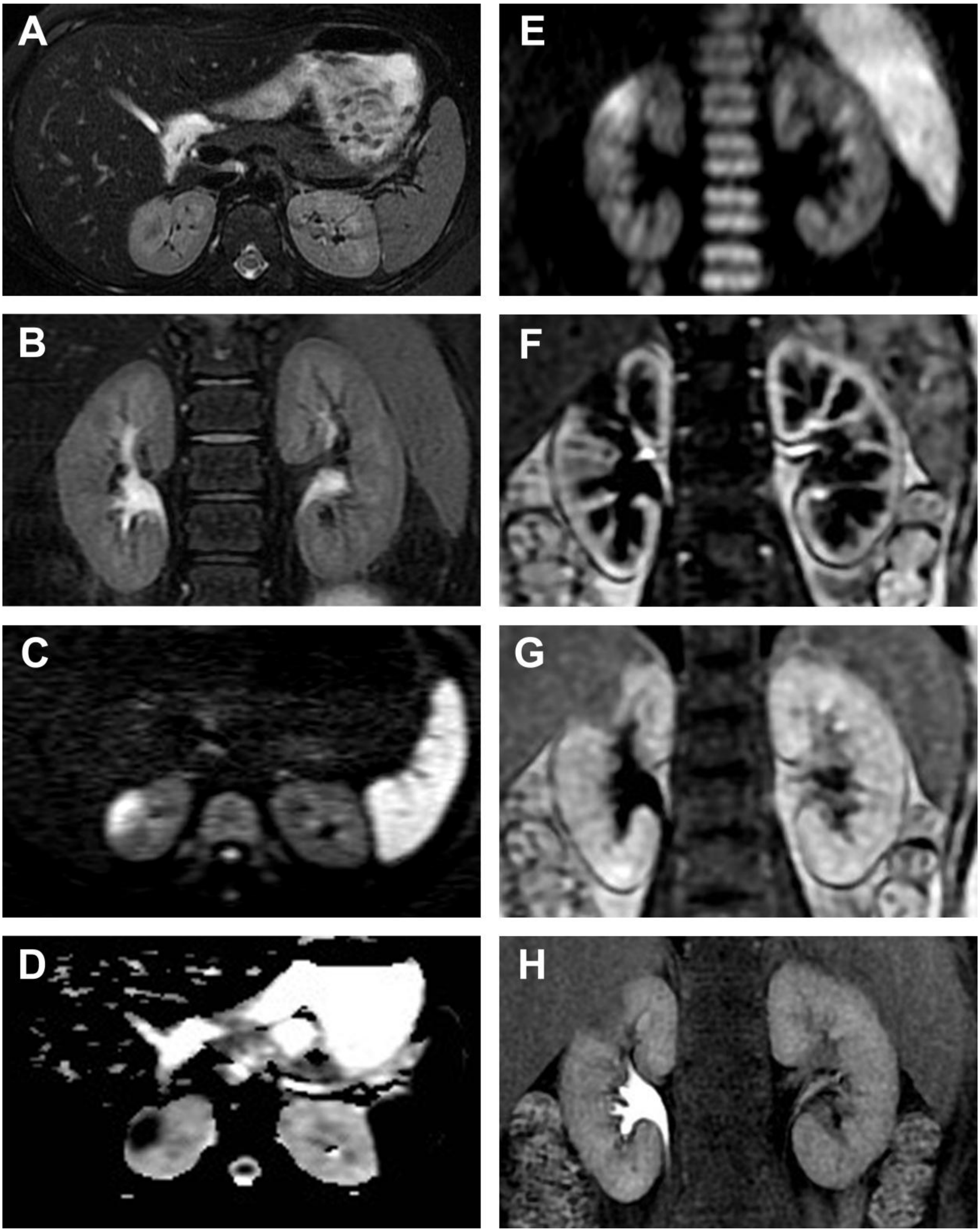
A
B
C
D
E
F
G
H

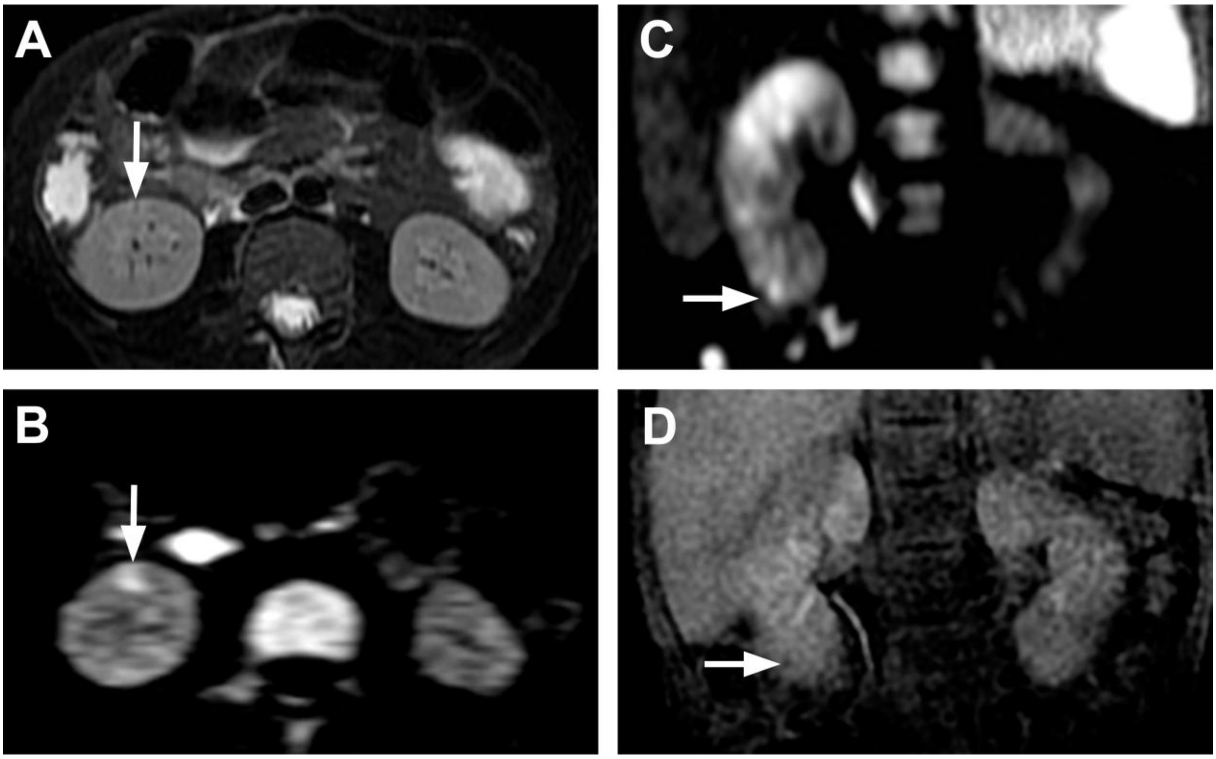
A
B
C
D

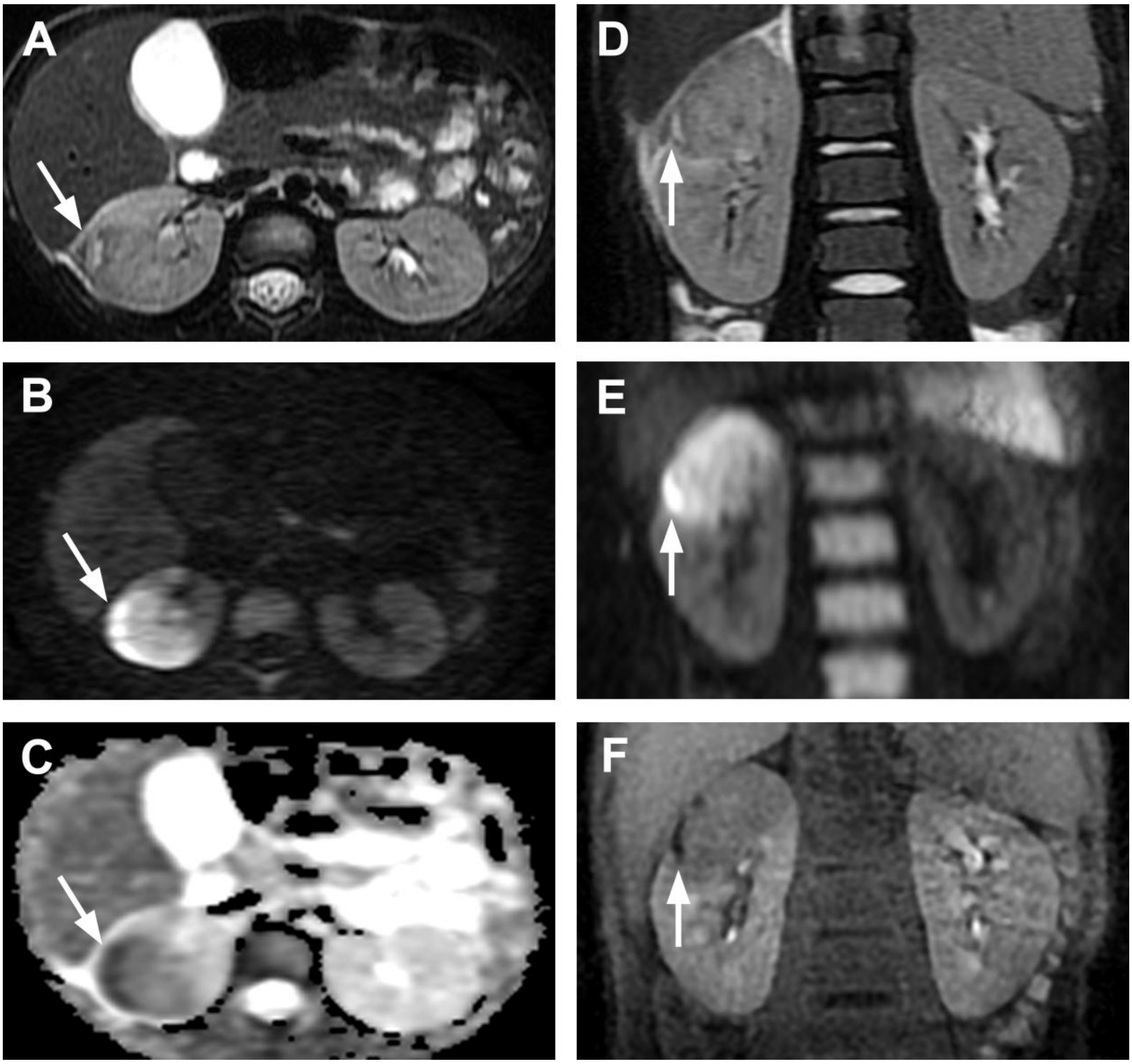
A
B
C
D
E
F